Special issue of the 2nd International Conference on Computational and Experimental Science and Engineering (ICCESEN 2015)

Effect of Dye Type on Montmorillonite-Supported Pr-Doped TiO_2 Composite Photocatalsyt

B. Otsukarci and Y. Kalpakli*

Yildiz Technical University, Department of Chemical Engineering, 34210, Istanbul, Turkey

Scarcity of water in today's world has led to scientific researches for finding smarter ways of discharging and re-using water located in the seas and lakes. That is how advanced oxidation technologies have emerged as one of the new discharging techniques to keep water sources clean. In our method we have synthesized praseodymium (Pr) doped TiO_2-Montmorillonite composite photocatalyst by using acid sol-gel method. Pr, in the group of rare earth metals, is known for its ability to form Lewis bases in order to break down aldehydes, amines, etc., by decreasing the crystal size and consequently increasing the surface area. We have used the mineral form of the bentonite clay (montmorillonite) to increase the surface area of our composite photocatalyst. Two types of azo dyes which are commercially known as Basic Yellow 28 (BY 28) and Basic Blue 41 (BB 41) were used in experimants. These dyes are composed of different chemical structures: BY 28 is known as azomethine dye (–CH=N–), whereas BB 41 has one azo bond (–N=N–). The initial model dye concentrations were 100 ppm. Amount of 1.0 g/l of photocatalyst was used throughout the experiments. In order to evaluate degradation efficiency results, the dissolved organic carbon analyzer was used. We have found the optimum dark adsorption time to be under 15 minutes. By stirring under 15 minutes in the dark we have achieved efficiency of 52.50% for BY 28 and 66.74% for BB 41. On the other hand, by stirring under UV-A light irradiation for two hours we have achieved the overall degradation efficiency of 86.30% for BY 28 and 92.39% for BB 41. Our results show that higher adsorption and overall efficiencies were observed in BB 41 than in BY 28. Moreover, according to Water Pollution Control Regulations, the chemical oxygen demand limitations for textile industry are between 200–400 mg/l. To evaluate the degradation characteristics of Pr-doped TiO_2-Montmorillonite composite, the change of chemical oxygen demand values with time for 100 mg/l of BY 28 and BB 41 were investigated. The obtained chemical oxygen demand values were 60.5 and 34.8 mg O_2/l after 2 hours of oxidation processes for BY 28 and BB 41. As it can be seen from the results, obtained values are below the limitations.

DOI: 10.12693/APhysPolA.129.198

PACS/topics: 81.16.Hc, 87.64.K, 87.64.km

1. Introduction

Recently, heterogeneous photocatalysis of TiO_2 doped with rare earth elements has attracted extensive attention due to broadening of the oxidation activity of TiO_2 into the visible region of spectrum, which decreases the cost of degradation and makes the process feasible for industrial usage. Even though TiO_2 has a large band gap (3.2 eV in the anatase form) and strong oxidation potential of the photogenerated holes ($\sim$ 2.9 V vs NHE at pH 0), its efficiency is limited under the visible light [1].

Photocatalytic reaction has several steps: (a) production of electron-hole pairs (e^-/h^+) by generating the required over-band-gap energy on the photocatalyst surface, (b) separation of e^-/h^+ pairs by electron scavengers or traps on TiO_2 surface, (c) a redox process between the separated e^- and h^+ and the pollutants located in the solution, (d) desorption of the products from the surface [2].

One of the ways to extend the visible light sensitivity spectrum of TiO_2 from UV area is to prolong the e^-/h^+ separation in order to have effective redox processes. Here is where the incorporation with rare earth elements becomes useful. Praseodymium, which is an element belonging to rare earth elements group, was used in this study as a doping agent. According to Xiuqin et al. doping of the photocatalyst with the appropriate amounts of rare earths improves the photocatalytic activity of the photocatalyst by increasing the formation rate of e^-/h^+ pairs and thus increasing the amount of hydroxyl radicals ($\cdot$OH) [3]. Su et al. have stated that doping with Pr induces the photocatalytic activity in visible range of spectrum [4].

In this study our aim was to prepare TiO_2-Montmorillonite (MMT) doped with Pr, using acid sol-gel method, in order to compare the degradation and decoloration results for two model pollutants. As the model pollutants, two colorants, Basic Yellow 28 (BY 28) and Basic Blue 41 (BB 41), were used. MMT, which is a mineral form of bentonite clay, widely found in Turkey, was used as the supporting material for TiO_2. Both, BY 28 and BB 41 are basic, cationic dyes soluble in water due to their sulfonate groups (SO_3^-) [5]. BY 28 is also known as the azomethine dye (-CH=N-) or the hydrazone dye (=N-N(H,R)-) [6]. BB 41 is a mono azo dye, due to presence in its structure of one azo group (-N=N-) [7]. BY 28 is used in acrylic, wool, and nylon dyeing [8]. BB 41 is suitable for acrylic, wool, and cotton dyeing [9].

*corresponding author; e-mail: kalpakli@yildiz.edu.tr

2. Experimental

BY 28 and BB 41 were purchased from Alptekim Dye and Chemicals Incorporated Company. The commercial name of BY 28 is Acryla Golden Yellow GL and the commercial name of BB 41 is Acryla Blue GRL. Pr-doped TiO_2-MMT has been synthesized using analytical grade precursors. These precursors were tetra-tert-buthyl-orthotitanate (Merck), absolute ethanol (Merck), nitric acid (Merck) and sodium bentonite (Esan Eczacıbaşı Industrial Raw Materials Incorporated Company, Kütahya). Praseodymium (III) nitrate hexahydrate 99.9% with a chemical formula of $Pr(NO_3)_3 \cdot 6H_2O$ was purchased from Sigma-Aldrich. Distilled water has been used in all experiments.

2.1. Equipment

All adsorption and photocatalytic oxidation experiments were conducted using Luzchem photoreactor. This reactor was equipped with eight UV-A black fluorescent 8 W lamps. Lamps were turned off during the adsorption experiments. WiseShake branded stirrer was used in the synthesis step. Dissolved organic carbon was analyzed using Hach-Lange IL 550 TOC-TN analyzer. In order to determine the effect of photocatalyst on the color properties of water, absorbance values after each experiment were measured using Perkin Elmer branded Lambda 35 UV/VIS spectrometer at $\lambda = 415$ nm for BY 28 and at $\lambda = 617$ nm for BB 41.

2.2. Experimental procedure

For the experiments we have employed solutions of 25 ml of BY 28 and BB 41 in a 100 ml beaker. Concentration was kept at 100 ppm throughout the experiments for both dyes. Optimum adsorption and degradation data was obtained step by step.

2.3. Adsorption process

As known from the previous experiments and literature findings, photocatalytic reactions take place collaboratively in two stages: adsorption and degradation. In the adsorption stage we have determined the optimum stirring conditions in the dark, when the UV lights were turned off, by trying stirring of BY 28 for 15, 25, 35, and 45 minutes.

2.4. Photocatalytic reactions

Degradation process was studied when we have determined our optimum adsorption time. Our aim was to obtain the lowest adsorption percentage and the highest oxidation potential. Our optimum adsorption time for BY 28 was 15 min. After that we have tried out different photocatalyst amounts of 1.0, 1.5, 2.0, 2.5, and 3.0 g/l under UV-A irradiation time of 35, 45, 60, 90, and 120 min. We have obtained the highest oxidation of BY 28, which had settled at around 120 min, using 1.0 g/l of photocatalyst. Later we have compared our results with those obtained for BB 41. In the experiments with BB 41 the degradation stage had lasted 30, 60, 90, and 120 min.

3. Results and discussion

3.1. Photocatalytic degradation experiments

Adsorption is an important step in the studied process, which increases the amount of compounds to be degraded under the UV-A irradiation. We have determined adsorption efficiencies for both dyes. After 15 min of absorption, the adsorption efficiency was 52.50% for BY 28 and 66.74% for BB 41. BB 41 had a higher adsorption capacity compared to BY 28. The highest overall efficiency (adsorption% + oxidation%, after 120 min of UV-A irradiation) was 86.30% for BY 28, which is less than that for BB 41, with a value of 92.39%.

When the UV-A irradiation time was increased from 30 to 120 min, the surface attacking rate for both dyes had decreased and finally had stabilized around the same value, as shown in Fig. 1. However, the initial attacking rate of BB 41 to the surface of the photocatalyst was higher. According to Bouafia et al. [10], who have applied the photo-Fenton process, the rate of oxidation of BB 41 was also higher than that of BY 28, which is coherent with our findings.

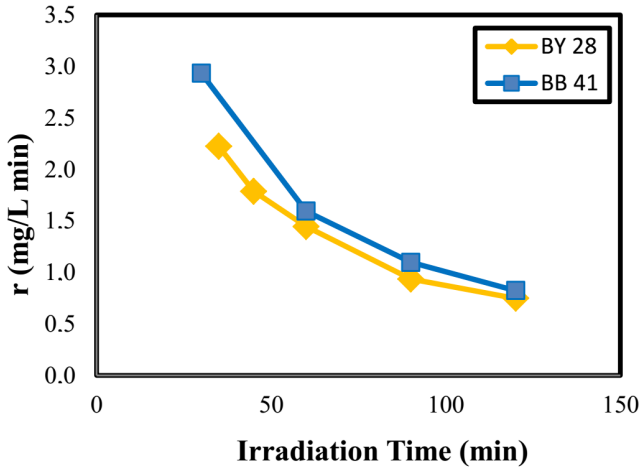


Fig. 1. Surface attack rate for BY 28 and BB 41 as function of UV-A irradiation time, after 15 min of dark adsorption. Concentration of the model compounds was 100 ppm. Amount of the photocatalyst used was 1.0g/l.

Kinetic results obtained by varying the irradiation time have shown that the 1st order Langmuir-Hinshelwood kinetics is applicable under these steady conditions. In this manner, values of the k_{apparent} and $t_{1/2}$ for BY 28 were were 0.0094 min^{-1} and 101.9 min, as shown in Table I. Even though photocatalyst attacked BB 41 faster due to higher adsorption yield reaction proceeded slower to reach its half-life value compared to BY 28.

Giwa et al. found apparent rate constant for 100 ppm of BB 41 as 0.005 l/mol min using only TiO_2 Degussa P-25 as a photocatalyst after 60 min of irradiation [11]. Our results are in a good agreement with the literature result.

TABLE I

Calculated apparent rate constant and half life values for BY 28 and BB 41 dyes.

	$k_{apparent}$ [min^{-1}]	$k_{apparent}$ [l/mol min]	$t_{1/2}$ [min]
BY 28	0.0068	0.0085	73.4
BB 41	0.0094	0.0055	101.9

After the degradation period, decolorization efficiency of dyes was observed as a function of time using a spectrophotometer.

3.2. UV-Vis spectroscopy

Degradation study of BY 28 and BB 41 was followed by a study using UV-Vis spectroscopy. The results are depicted in Fig. 2. Discoloration efficiency (%) for the BB 41 was lower than that of BY 28 at the end of 2 h of irradiation. However, at the end of 90 min period of irradiation BB 41 had reached its highest discoloration efficiency. Therefore, the highest discoloration efficiencies calculated at the end of 2 h for BY 28 and 90 min for BB 41 were 84.05% and 80.94%, respectively. This is due to the different chemical structures of the dyes.

As the overall efficiency had increased, the absorbance values for discoloration of the dyes had eventually decreased after 120 min of illumination, as shown in Fig. 2. In Fig. 2a TOC removal efficiency has a sigmoidal shape, indicating the formation of by-products that slow down the degradation efficiency and the degradation rate calculated in Table I for BY 28 [12].

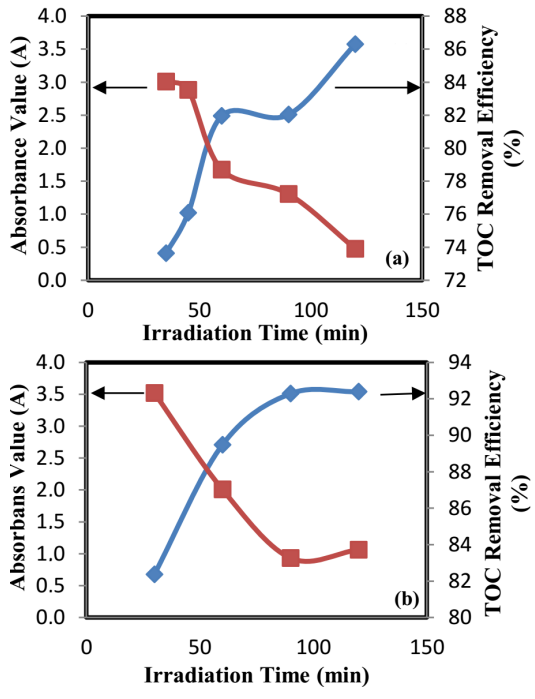


Fig. 2. Comparison of the change of the TOC removal (blue) and the remaining dye absorbance value (red) with the irradiation time, for two model dyes (a) BY 28 and (b) BB 41.

3.3. FTIR

At the end of the study, the characteristic peaks of BY 28 and BB 41 were investigated using FTIR analysis. For BY 28 these characteristic peaks were found at 1638, 1604, 1552, 1328, 1178, 935, 829, 786, and 642 cm^{-1}, as shown in Fig. 3. In an orderly fashion peak at 1638 cm^{-1} is related to stretching of the C=N group, due to hydrazine form of the dye [13], peak at 1604 cm^{-1} is related to vibration of the C=N group [14], 1552 cm^{-1} is related to combined vibration of NH–N=C group's N–H bending and –N=C stress [15], peaks from the range of 1550–1300 cm^{-1}, 1463, and 1330 cm^{-1} belong to the alkanes and alkenes [16], 1247 cm^{-1} from the range of 1300–1000 cm^{-1} belongs to the ethers [16], 1178, 1120, and 1034 cm^{-1} peaks belong to the S=O stress due to RO–SO_3^- [16], 935 and 829c m^{-1} peaks belong to the C–H bending vibrations, located in the range of 950–780 cm^{-1} [17, 18].

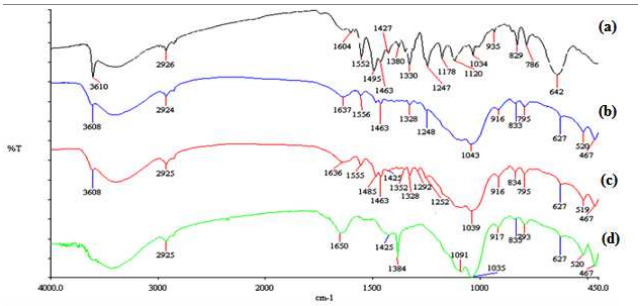


Fig. 3. Comparision of FTIR results for BY 28. (a) BY 28 dye powder, (b) 15 min adsorption, (c) 15 min adsorption + oxidation (d) 1% Pr, 25% TiO_2-MMT composite photocatalyst.

Range 1300–900 cm^{-1} in the spectrum belongs to the aromatics group in the composition of the dye, which is removed from the solution with the sequential adsorption and degradation reactions. In addition, peaks at 935 and 642 cm^{-1} also disappear. A characteristic peak at 1604 cm^{-1} was also cleared away at the end of redox reactions.

Peak at 3610 cm^{-1}, which is the characteristic peak of the photocatalyst, due to OH stretching reduced BY 28 dye powder's 3610 cm^{-1} peak represented by the C–H bending.

Characteristic peaks of mono azo dye BB 41 were also analyzed. For BB 41 these characteristic peaks are located at 1610, 1547, 1483, 1426, 1402, 1372, 1328, 1268, 1110, 984, 860, 829, and 732 cm^{-1}, as shown in Fig. 4. Peak at 1610 cm^{-1} belongs to the amines and amides represented by the range of 1650–1550 cm^{-1} [16], peaks at 1547, 1483, 1426, and 1402 cm^{-1} are related with the N=N vibration, represented by the 1500–1400 cm^{-1} range [19], peaks at 1372, 1328, and 1268 cm^{-1} are due to symmetric C–O stretching [14], 1114 cm^{-1} is related to stretching of S=O, due to RO–SO_3^- group [16], peak at 987 cm^{-1} belongs to the alkenes and aromatics in the

range of 1000–650 cm^{-1} [16], peaks at 860 and 829 cm^{-1} from the range of 950–780 cm^{-1} are related with the C–H bending [19] and to the range of 800–400 cm^{-1}, due to aromatic compounds [16].

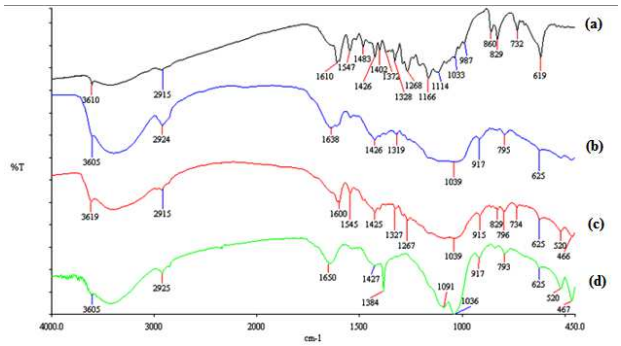


Fig. 4. Comparision of FTIR results for BB 41. (a) BB 41 dye powder, (b) 15 min adsorption, (c) 15 min adsorption + oxidation (d) 1% Pr, 25% TiO_2-MMT composite photocatalyst.

When 1300–950 cm^{-1} range is investigated, it is seen that, due to sequential reactions of adsorption and oxidation, the aromatic compounds, peaks of which are located in this area, are removed. Therefore, peaks at 1166, 1114, and 987 cm^{-1} are reduced at the end of reactions. In the range of 1700–1270 cm^{-1} peaks at 1483, 1402, and 1372 cm^{-1}, resulted from C=N bond due to aromatic compounds, amines, alkanes, and alkenes, are also degraded. Peaks at 860, 829, 732, 619 cm^{-1} are also removed by the sequential adsorption and oxidation reactions.

4. Conclusions

In this study degradation and decoloration of two basic cationic azo dyes were investigated as a function of irradiation time. This work demonstrates for the first time that MMT-supported Pr-doped TiO_2 composite photocatalyst has a high efficiency for both degradation and decoloration. The degradation and decoloration rates of the dyes and their efficiencies were influenced by the time the dyes were exposed to the UV-A light. Highest TOC removal achieved for BY 28 and BB 41 were 86.30% and 92.39% at 120 min respectively. Whereas the most discoloration efficiency was achieved at the end of 2 h with 84.05% for BY 28, the highest discoloration rate for BB 41 was achieved at the end of 90 min with 80.94%. Even though, production of by-products in the degradation reaction of BY 28 is observed, the system is fast enough to overcome inhibition of oxidation and continues the photocatalytic reaction.

FTIR analysis helped us to determine the characteristic peaks of BY 28 and BB 41 and had shown that most of the dye removal is achieved only after 2 h of irradiation. FTIR analysis results supported the results of TOC and UV-Vis analysis. The most important part of this report is the conduction of the experiments without using oxidation agents. In the further experiments oxidation agents will be used to improve degradation and discoloration efficiencies in a shorter irradiation time.

Acknowledgments

The authors would like to thank Yıldız Technical University BAPK project no. 2014-07-01-YL05 for financial support of this work.

References

[1] C. Anderson, A. Bard, *J. Phys. Chem.* **99**, 9882 (1995).

[2] A. Wold, *Chem. Mater.* **5**, 280 (1993).

[3] O. Xiuqin, M. Junping, W Qimin, Y. Junmei, *J. Rare Earth* **24**, 251 (2006).

[4] W. Su, J. Chen, L. Wu, X. Wang, X. Wang, X. Fu, *Appl. Catal. B: Environmental* **77**, 264 (2008).

[5] V. Augugliaro, C. Baiocchi, A.B. Prevot, E. Garcia-Lopez, V. Loddo, S. Malato, G. Marci, L. Palmisano, M. Pazzi, E. Pramauro, *Chemosphere* **49**, 1223 (2002).

[6] V. Djokic, J. Vujovic, A. Marinkovic, R. Petrovic, D. Janackovic, A. Onjia, D. Mijin, *J. Serbian Chem. Soc.* **77**, 1747 (2012).

[7] W.Z. Tang, H. An, *Chemosphere* **31**, 4157 (1995).

[8] K. Marungrueng, P. Pavasant, *J. Environ. Management* **78**, 268 (2006).

[9] Z. Rashedi, S.R. Setayesh, S. Ghasemi, M.R. Gholami, *4th International Comference on Nanostructures, 12-14 March*, 2012, p. 1002.

[10] S. Bouafia-Chergui, N. Oturan, H. Khalaf, M. Oturan, *Procedia Eng.* **33**, 181 (2012).

[11] A. Giwa, P.O. Nkeonye, K.A. Bello, K.A. Kolawole, *J. Environ. Protect.* **3**, 1063 (2012).

[12] I.K. Konstantinou, T.A. Albanis, *Appl. Catal. B: Environmental* **49**, 1 (2004).

[13] H. Khanmohammadi, M. Erfantalab, *Spectrochim. Acta A* **86**, 39 (2012).

[14] M. Stylidi, D.I. Kondarides, X.E. Verykios, *Appl. Catal. B: Environmental* **40**, 271 (2003).

[15] C.W.M. Yuen, S.K.A Ku, P.S.R. Choi, C.W. Kan, S.Y. Tsang, *RJTA* **9**, 26 (2005).

[16] A. Altun, K. Gölcük, M. Kumru, *J. Mol. Struct.: THEOCHEM* **637**, 155 (2003).

[17] K. Chaitanya, *Spectrochim. Acta A* **86**, 159 (2012).

[18] H. Karaer, İ.E. Gümrükçüoğlu, *Turkish J. Chem.* **23**, 67 (1999).

[19] N. Karthikeyan, J.J. Prince, S. Ramalingam, S. Periandy, *Spectrochim. Acta A* **139**, 229 (2015).